Clemson University
TigerPrints

All Theses | Theses

5-2008

Improved closed-form bounds on the performance of convolutional codes with correlated Rayleigh fading

Dwight Hutchenson
Clemson University, dhutche@ces.clemson.edu

Follow this and additional works at: https://tigerprints.clemson.edu/all_theses

 Part of the Electrical and Computer Engineering Commons

Recommended Citation
Hutchenson, Dwight, "Improved closed-form bounds on the performance of convolutional codes with correlated Rayleigh fading" (2008). *All Theses*. 326.
https://tigerprints.clemson.edu/all_theses/326

This Thesis is brought to you for free and open access by the Theses at TigerPrints. It has been accepted for inclusion in All Theses by an authorized administrator of TigerPrints. For more information, please contact kokeefe@clemson.edu.

IMPROVED CLOSED-FORM BOUNDS ON THE PERFORMANCE OF CONVOLUTIONAL CODES WITH CORRELATED RAYLEIGH FADING

A Thesis
Presented to
the Graduate School of
Clemson University

In Partial Fulfillment
of the Requirements for the Degree
Master of Science
Electrical Engineering

---

by
Dwight Keith Hutchenson
May 2008

Accepted by:
Dr. Daniel L. Noneaker, Committee Chair
Dr. Michael B. Pursley
Dr. Carl W. Baum

ABSTRACT

New bounds on the probability of bit error are presented for a coded communication system with binary antipodal modulation and soft-decision maximum-likelihood decoding over a correlated Rayleigh-fading channel. The bounds are closed-form expressions in terms of the code's transfer function; they are illustrated by considering a system using convolutional encoding. A long-standing conjecture regarding the worst-case error event in correlated Rician fading is proven for the special case of correlated Rayleigh fading, and it is used in the development of some of the new bounds. The bounds are shown to be tighter than previously developed closed-form bounds for communications using convolutional codes in correlated Rayleigh fading.

DEDICATION

In loving memory of my grandfather, Rev. James C. Hunnicutt, whose wisdom, faith, and work ethic continue to inspire me.

ACKNOWLEDGMENTS

I would like to sincerely thank my advisor, Dr. Daniel Noneaker, for his generous support throughout my undergraduate and graduate studies. His insight and direction were invaluable to the development and preparation of this thesis. I would also like to thank Dr. Michael Pursley and Dr. Carl Baum for taking the time to serve on my thesis committee. Their feedback was greatly appreciated. I should also mention that this research was made possible through the financial assistance of the U.S. Army Research Office and the U.S. Army Research Laboratory, for which I am very grateful.

I would be remiss if I failed to acknowledge my parents, Keith and Brenda Hutchenson, for without their unwaivering support and guidance through the years, I surely would not be where I am today. And, of course, I would like to thank my lovely wife, Holly, who has helped me in countless ways, and with whom I look forward to spending the next chapter in my life.

TABLE OF CONTENTS

Table of Contents (Continued)

Page

LIST OF FIGURES

CHAPTER 1

INTRODUCTION

Many communication systems employ code-symbol interleaving to minimize the effect of channel memory on the decoding of a message received over a fading channel. If the interleaving depth is sufficiently large in relation to the rate of fading in the channel, the effect of the channel on the decoder performance for a trellis code can be accurately approximated as independent fading of channel symbols into the decoder. For many scenarios of practical interest, the independence approximation is overly optimistic, however, and the effect of finite interleaving depth must be accounted for in the evaluation of system performance.

The instance of this problem that has received the greatest attention in past research concerns the performance of a system with convolutional coding and binary antipodal modulation, a Rayleigh-fading channel, and soft-decision maximum-likelihood sequence detection (Viterbi decoding) at the receiver. Several approaches have been employed to obtain expressions for an upper bound on the average probability of bit error in this circumstance. For any error event of the code, the exact pairwise error-event probability can be expressed in closed form in terms of the eigenvalues of the associated channel covariance matrix [1].

The closed-form expressions for pairwise error-event probabilities can be used in turn to express the union bound on the average probability of bit error or first event error as an infinite series. (For example, see numerous references cited in [2].) The

series can not be expressed in a closed form, however; thus in practice it can be used only to determine a partial sum that is an approximation to the union bound. A partial sum determined in this way does not necessarily yield an upper bound on the average probability of bit error.

A closed-form expression for an upper bound on the probability of error can be obtained using any closed-form upper bound on the pairwise error-event probability that is a linear combination of geometric functions of the Hamming weight of the error event. The function can be employed with flow-graph techniques to obtain a transfer-function bound on the union bound (and thus on the average probability of error) [3]. This approach has been employed for convolutional coding and independent Rayleigh fading to obtain a transfer-function bound based on the Chernoff bound on the pairwise error-event probability[4] or an improvement of the Chernoff bound [5].

The same approach has been used to obtain transfer-function bounds for convolutional coding and correlated Rayleigh fading [6, 7]. A fading-channel model that is commonly used in system analysis employs an exponential time-correlation function for the correlated Rayleigh fading, which results in a zero-mean, first-order Gauss-Markov channel. The exponentially correlated Rayleigh-fading channel is among those considered in [6], and it is the sole focus of [7].

A closed-form expression for the exact union bound on the average probability of bit error is developed in [8] in terms of a single-dimensional improper integral and in [9] in terms of a single-dimensional proper integral. Either can be evaluated accurately with numerical techniques of reasonable complexity. The results in both

papers are limited to channels with *independent* fading, however.

In this thesis we develop several new, simple bounds on the pairwise error-event probability for communications in correlated Rayleigh fading with an arbitrary time-correlation function. For the channel with exponentially correlated fading and an error event of a given Hamming weight and an arbitrary spacing of channel symbols, we show that the pairwise error-event probability and its Chernoff bound are no greater than the corresponding values for an error event of the same Hamming weight and minimum spacing of symbols. We also develop improved, closed-form upper bounds on the average probability of bit error for soft-decision maximum-likelihood sequence detection of a convolutional code with correlated Rayleigh fading and perfect channel-state information at the receiver. Our new results for the pairwise error-event probability and the average probability of bit error can be adapted to yield similar bounds for uniform trellis codes. The results for the pairwise error-event probability are also directly applicable to performance analysis for uncoded diversity signaling. They may also prove useful in the analysis of performance for other communication systems, including those using turbo codes and space-time codes.

The system and channel are described in Chapter 2. Previous results giving an expression for the exact pairwise error-event probability are reviewed in Chapter 3. In Chapter 4, we develop improved geometric-form bounds and related integral bounds on the pairwise error-event probability for a general correlated channel. Further results on the pairwise error-event probability that are specific to the exponentially correlated channel are developed in Chapters 5 and 6. The results of Chapter 5 are

used in Chapter 7 to obtain several new transfer-function bounds on the average probability of bit error. Examples are considered in Chapter 8 to illustrate the improvement the new bounds provide over the best previously developed closed-form bound, and conclusions are summarized in Chapter 9.

CHAPTER 2

SYSTEM AND CHANNEL MODELS

Each binary code word $\underline{c} = (c_1, c_2, ..., c_L)$ from the convolutional encoder is passed through an arbitrary interleaver of designed interleaving depth m. The resulting binary sequence at the output of the interleaver $\underline{\tilde{c}} = (\tilde{c}_1, \tilde{c}_2, ..., \tilde{c}_L)$, which is transmitted using binary antipodal modulation. The channel is piecewise-constant with additive white Gaussian noise. The baseband-equivalent received signal is given by

$$r(t) = \sqrt{\frac{E_c}{T}} \sum_{k=1}^{L} \tilde{\alpha}_k (-1)^{\tilde{c}_k} \psi_T(t - kT) + n(t),$$

where $n(t)$ is the white Gaussian noise process with double-sided, baseband-equivalent power spectral density of $N_0/2$. The channel-symbol duration is T, and $\psi_T(t)$ is a complex pulse of unit average power that is time-limited to $[0, T)$.

The baseband-equivalent channel gain $\tilde{\alpha}_k$ during the kth channel-symbol interval is a complex-valued, zero-mean Gaussian random variable with unit variance. Thus the average energy per received channel symbol is E_c, and the channel-symbol signal-to-noise ratio in the received signal is

$$\text{SNR} = \frac{E_c}{N_0}.$$

In Chapters 3 and 4, an arbitrary autocorrelation function is considered for the discrete-time Gaussian random process $(\tilde{\alpha}_1, \ldots, \tilde{\alpha}_L)$. In Chapters 5-8, attention is

restricted to a channel that has the autocorrelation function given by

$$\mathrm{Cov}(\tilde{\alpha}_k, \tilde{\alpha}_j) = \exp(-2\pi|k-j|B_dT),$$

however. The latter discrete-time random process thus has a geometric time-correlation function, and it characterizes the piecewise-constant approximation to the Rayleigh-fading channel with an exponential time-correlation function and Doppler spread B_d [10]. In keeping with common usage (e.g, [7]), in this thesis the piecewise-constant channel is referred to as the exponentially correlated channel. The *normalized Doppler spread* of the channel is defined as $D_T \triangleq B_dT$.

The complex correlator output for the kth code symbol at the receiver is the code-symbol statistic

$$\tilde{Z}_k = \int_{kT}^{(k+1)T} r(t)\psi_T^*(t-kT)\,\mathrm{d}t = \sqrt{E_cT}\tilde{\alpha}_k(-1)^{\tilde{c}_k} + N_k,$$

where (N_k) are i.i.d. zero-mean, complex-valued Gaussian random variables with variance $N_0T/2$. The correlator outputs are deinterleaved prior to decoding. The sequence of statistics at the output of the deinterleaver (going into the decoder) is denoted by $(Z_1, \ldots, Z_L)$, which corresponds to the original ordering of code symbols in $\underline{c}$. The corresponding reordered channel gains are similarly denoted by $(\alpha_1, \ldots, \alpha_L)$. Maximum-likelihood sequence detection is used at the receiver based on the code-symbol statistics and perfect estimates of the channel gains. Thus the correlator

form of the path metric is given by

$$M(\underline{c}) \;=\; \sum_{k=1}^{L} Re\{(-1)^{c_k}\alpha_k^* Z_k\},$$

and the sequence detector chooses the code sequence with the largest path metric.

It is desired that consecutive code-symbol statistics into the decoder correspond to channel symbols that are transmitted at least m channel-symbol intervals apart, and a well-designed interleaver ensures that this objective (the *designed interleaver depth*) is achieved over any span corresponding to low-weight error events in the code. Interleavers of practical utility are periodic interleavers [11]. Periodic interleavers include rectangular block interleavers (defined in Section 8.1) and convolutional interleavers [12] (referred to as "periodic interleavers" therein), among others. No practical periodic interleaver can achieve any designed interleaving depth greater than one over all code-symbol spans; thus each periodic interleaver achieves its design objective only approximately.

In this thesis, we use the approximation that the designed interleaver depth m is achieved over all code-symbol spans so that any two code-symbol statistics Z_j and Z_k correspond to channel symbols transmitted $m|j-k|$ symbol intervals apart. We refer to this as the *ideal periodic-interleaving model*, for which

$$\mathrm{Cov}(\alpha_k, \alpha_j) = \exp(-2\pi m|k-j|D_T). \tag{2.1}$$

For convenience we define the *covariance parameter* of the system as

$$q \triangleq \exp(-2\pi m D_T).$$

Thus

$$\mathrm{Cov}(\alpha_k, \alpha_j) = q^{|k-j|}. \tag{2.2}$$

CHAPTER 3

EVALUATION OF THE PAIRWISE ERROR-EVENT PROBABILITY

The pairwise error-event probability at the decoder output can be expressed in a closed form as shown in [13]. This chapter summarizes the development in that earlier paper and defines notation used in our development of new results presented in the subsequent chapters. In the remainder of the thesis, assume without loss of generality that $\underline{c}$ is the all-zeros code sequence. Let $\hat{\underline{c}}$ represent a code sequence of length L with Hamming weight d. The receiver chooses $\hat{\underline{c}}$ over $\underline{c}$ if $M(\hat{\underline{c}}) > M(\underline{c})$. Therefore, if $\underline{c}$ is the transmitted code sequence, the conditional pairwise error-event probability given $\underline{\alpha}$ for the sequence $\hat{\underline{c}}$ is

$$P(\hat{\underline{c}}, \underline{\alpha}) \;=\; P\left\{\sum_{k=1}^{L} Re\{|c_k - \hat{c}_k|\alpha_k^* Z_k\} < 0\right\}.$$

For convenience, let $\underline{A} = \{\alpha_{i_1}, \cdots, \alpha_{i_d}\}$ correspond to the d positions of the erroneous code symbols in $\hat{\underline{c}}$. Conditioned on $\underline{A}$, the statistics $\{Z_{i_1}, \cdots, Z_{i_d}\}$ are independent, complex-valued, Gaussian random variables. Thus the conditional pairwise error-event probability given $\underline{A}$ is given by

$$P(\hat{\underline{c}}, \underline{A}) \;=\; Q\left(\sqrt{\frac{2E_c}{N_0}\sum_{k=1}^{d}|A_k|^2}\right). \tag{3.1}$$

Let $\Sigma_A = E[\underline{A}\,\underline{A}^H]$ denote the covariance matrix of $\underline{A}$; it is referred to as the *channel covariance matrix* for the corresponding error event. Since Σ_A is Hermitian,

it can be represented by its spectral decomposition [14, Theorem 5.2.1]

$$\Sigma_A = U\Lambda U^H.$$

The matrix U is unitary, and $\Lambda = \text{diag}\{\lambda_1, \ldots, \lambda_d\}$ where (λ_k) are the eigenvalues of Σ_A where, without loss of generality, $0 \leq \lambda_1 \ldots \leq \lambda_d$. (The eigenvalues are nonnegative since Σ_A is nonnegative definite.) If

$$\underline{Y} \triangleq U^H \underline{A},$$

it follows that

$$\underline{Y}^H \underline{Y} = (U^H \underline{A})^H U^H \underline{A} = \underline{A}^H \underline{A},$$

and the covariance matrix of Y is

$$\begin{aligned} \Sigma_Y &= E[U^H \underline{A}(U^H \underline{A})^H] \\ &= U^H \Sigma_A U \\ &= \Lambda. \end{aligned}$$

Thus $\text{Var}[Y_k] = \lambda_k$ for $1 \leq k \leq d$. Since $\Sigma_Y = \Lambda$ is diagonal, the random variables $\{Y_1, \ldots, Y_d\}$ are uncorrelated and thus independent (since they are jointly Gaussian). Therefore, we can replace $\sum_{k=1}^d |A_k|^2$ in (3.1) with $\sum_{k=1}^d |Y_k|^2$, which replaces a sum of correlated random variables with a sum of independent random variables.

We define

$$V_k \triangleq \frac{2E_c}{N_0}|Y_k|^2,$$

which has an exponential distribution with probability density function

$$f_{V_k}(v) = \frac{1}{2\lambda_k E_c/N_0} \exp\left(-\frac{v}{2\lambda_k E_c/N_0}\right),$$

and moment generating function

$$\Phi_{V_k}(s) = \frac{1}{2\lambda_k E_c/N_0}\left(\frac{1}{2\lambda_k E_c/N_0} - s\right)^{-1}.$$

If $X \triangleq \sum_{k=1}^{d} V_k$, then the moment generating function of X is

$$\Phi_X(s) = \prod_{k=1}^{d} \Phi_{V_k}(s).$$

Once a partial fraction expansion is performed on $\Phi_X(s)$, the probability density function of X, $f_X(x)$, is readily obtained. The pairwise error-event probability can now be expressed as

$$P(\hat{\underline{c}}) = \int_{x=0}^{\infty} Q(\sqrt{x}) f_X(x)\,\mathrm{d}x. \tag{3.2}$$

A closed-form expression for (3.2) is obtainable, but the form of the expression depends on the number and multiplicity of the distinct eigenvalues. The closed-form expression for the pairwise error-event probability is given below for two special cases.

Special Case 1: $\lambda_k = \lambda$ for $1 \leq k \leq d$

The trace of a matrix is not changed by a diagonalizing transformation. Therefore, $\sum_{k=1}^{d} \mathrm{Var}(Y_k) = \sum_{k=1}^{d} \mathrm{Var}(A_k) = d$, which for this case implies that each Y_k has unit variance. Thus X is a gamma-distributed random variable, and its probability density function is

$$f_X(x) = \frac{x^{d-1}}{\Gamma(d)(2E_c/N_0)^d} \exp\left(-\frac{x}{2E_c/N_0}\right)$$

for $x \geq 0$. Substitution of this expression into (3.2), followed by standard techniques of integration, results in

$$P(\hat{\underline{c}}) = \frac{1}{2} - \frac{1}{2}\sqrt{\frac{E_c/N_0}{1+E_c/N_0}} \sum_{i=1}^{d} \binom{2i}{i} \left[4(1+E_c/N_0)\right]^{-i}. \tag{3.3}$$

Special Case 2: $\{\lambda_1, \ldots, \lambda_d\}$ are distinct

The probability density function of X is given by

$$f_X(x) = \frac{1}{2} \sum_{i=1}^{d} \left(\prod_{j \neq i} \frac{\gamma_i}{\gamma_i - \gamma_j} \right) \frac{1}{\gamma_i} \exp\left(-\frac{x}{2\gamma_i}\right),$$

for $x \geq 0$. Substitution into (3.2) and standard techniques of integration yield

$$P(\hat{\underline{c}}) = \frac{1}{2} \sum_{i=1}^{d} \left(\prod_{j \neq i} \frac{\lambda_i}{\lambda_i - \lambda_j} \right) \left[1 - \sqrt{\frac{\lambda_i E_c/N_0}{1+\lambda_i E_c/N_0}} \right].$$

CHAPTER 4

BOUNDS ON THE PAIRWISE ERROR-EVENT PROBABILITY FOR THE GENERAL CORRELATED CHANNEL

In Chapter 7, bounds on the pairwise error-event probability are used to determine new transfer-function bounds on the probability of bit error. This requires a bound on the pairwise error-event probability that is a linear combination of geometric functions of the Hamming weight of the error event. New bounds of this type are developed in this chapter which serve as intermediate results for use in Chapter 7. In the following chapters, $P(\Sigma)$ is used to denote the pairwise error-event probability for the error event with channel covariance matrix Σ in order to emphasize its dependence on Σ. Similarly, $P_C(\Sigma)$ is used to denote the Chernoff bound on the same probability.

4.1 Rational-Polynomial Bounds

The random variables (V_k) are independent; thus, the pairwise error-event probability can be expressed as

$$P(\Sigma_A) = \int_{v_d=0}^{\infty} \dots \int_{v_1=0}^{\infty} Q(\sqrt{v_1 + \dots + v_d})\, f_{V_1}(v_1) \dots f_{V_d}(v_d)\, \mathrm{d}v_1 \dots \mathrm{d}v_d. \qquad (4.1)$$

Substituting the upper bound

$$Q(x) \leq \frac{1}{2} \exp(-x^2/2),$$

for $x \geq 0$, from [3] into (4.1) yields the Chernoff bound

$$P(\Sigma_A) \leq P_C(\Sigma_A) = \frac{1}{2} \prod_{k=1}^{d} (1 + \lambda_k E_c/N_0)^{-1}, \tag{4.2}$$

as in [7, equation (7)]. A geometric-form upper bound on the pairwise error-event probability is obtained from any non-negative lower bound λ_{lb} on the eigenvalues of Σ_A. Since $\lambda_{lb} \leq \lambda_k$ for all k, it follows from (4.2) that

$$P(\Sigma_A) \leq \frac{1}{2}(1 + \lambda_{lb} E_c/N_0)^{-d} \tag{4.3}$$

as in [7, equation (9b)].

A new geometric-form upper bound on the pairwise error-event probability is obtained from any non-negative lower bound λ_{lb} and any upper bound λ_{ub} on the eigenvalues of Σ_A. Its development uses the following lemma.

Lemma 4.1. *Suppose* $0 \leq \lambda_{lb} \leq \lambda_{ub}$ *and* $C \geq 0$. *For any* x, $0 \leq x \leq 1$,

$$(1 + \lambda^* C)^{-1} \leq (1 + \lambda_{lb} C)^{-x} (1 + \lambda_{ub} C))^{-(1-x)}, \tag{4.4}$$

where

$$\lambda^* = x\lambda_{lb} + (1 - x)\lambda_{ub}.$$

Proof: Let $\phi(z) = \log[(1 + zC)^{-1}]$, for $z > 0$. The second derivative of $\phi(z)$ is $\phi''(z) = C^2(1 + zC)^{-2}$, which is strictly positive. Therefore, $\phi(z)$ is convex, and by

Jensen's inequality [15],

$$\phi(\lambda^*) \leq x\,\phi(\lambda_{lb}) + (1-x)\,\phi(\lambda_{ub}).$$

Replacing $\phi(z)$ with $\log[(1+zC)^{-1}]$ we obtain

$$\log[(1+\lambda^* C)^{-1}] \leq \log[(1+\lambda_{lb}C)^{-x} \cdot (1+\lambda_{ub}C)^{-(1-x)}].$$

Taking the anti-logarithm of both sides of the inequality results in (4.4). □

Lemma 4.1 is used in the proof of the new bound, which is given as the following theorem.

Theorem 4.1.

$$P(\Sigma_A) \leq \left[(1+\lambda_{lb}E_c/N_0)^{-y}\,(1+\lambda_{ub}E_c/N_0)^{-(1-y)}\right]^d, \tag{4.5}$$

where $0 \leq y \leq 1$ *and satisfies*

$$1 = y\lambda_{lb} + (1-y)\lambda_{ub}.$$

Proof: Let x_k satisfy $\lambda_k = x_k\lambda_{lb} + (1 - x_k)\lambda_{ub}$. Applying Lemma 4.1 with $C = E_c/N_0$ to (4.2), we have

$$\begin{aligned} P(\Sigma_A) &\leq \prod_{k=1}^{d}(1 + \lambda_{lb}E_c/N_0)^{-x_k}(1 + \lambda_{ub}E_c/N_0)^{-(1-x_k)} \\ &= \left[(1 + \lambda_{lb}E_c/N_0)^{-y}\,(1 + \lambda_{ub}E_c/N_0)^{-(1-y)}\right]^d, \end{aligned}$$

where $y = \frac{1}{d}\sum_{k=1}^{d} x_k$. Because the trace of a matrix is equal to the sum of its eigenvalues and $\mathrm{tr}\{\Sigma_A\} = d$, we know that

$$d = \sum_{k=1}^{d}\lambda_k = \sum_{k=1}^{d}(x_k\lambda_{lb} + (1 - x_k)\lambda_{ub}).$$

Dividing by d, we see that y must satisfy $1 = y\lambda_{lb} + (1-y)\lambda_{ub}$ and that $\lambda_{lb} \leq 1 \leq \lambda_{ub}$. Thus $0 \leq y \leq 1$. □

An example of lower and upper bounds λ_{lb} and λ_{ub} applicable to any covariance matrix Σ_A are those obtained from Geršgorin's Theorem [14, Theorem 10.6.1], though the resulting lower bound λ_{lb} is useful (positive) only if the matrix is strictly diagonally dominant [14, page 373].

4.2 Integral Bounds

In this section, the generalization to correlated Rayleigh fading of an equality developed in [9] is used in developing further bounds. The function $Q(x)$ can be

expressed as the proper integral [9]

$$Q(x) = \frac{1}{\pi} \int_{\theta=0}^{\pi/2} \exp\left(\frac{-x^2}{\sin^2\theta}\right) \, \mathrm{d}\theta.$$

Use of this representation in (4.1) (followed by a change of the order of integration) results in an exact proper-integral expression for the pairwise error-event probability

$$P(\Sigma_A) = \frac{1}{\pi} \int_{\theta=0}^{\pi/2} \prod_{k=1}^{d} \left[\frac{\sin^2\theta}{\sin^2\theta + \lambda_k E_c/N_0}\right] \, \mathrm{d}\theta \tag{4.6}$$

as in [16, equation (7)]. The two approaches considered in the previous section can be mimicked here to obtain integral bounds that are appropriate for use with the code's transfer function.

The first upper bound is obtained by noting that $(\sin^2\theta + \lambda_{lb} E_c/N_0)^{-1} \geq (\sin^2\theta + \lambda_k E_c/N_0)^{-1}$ for all k so that

$$P(\Sigma_A) \leq \frac{1}{\pi} \int_{\theta=0}^{\pi/2} \left[\frac{\sin^2\theta}{\sin^2\theta + \lambda_{lb} E_c/N_0}\right]^d \, \mathrm{d}\theta \tag{4.7}$$

following [17, equation (22)]

Application of Lemma 4.1 with $C = E_c/(N_0 \sin^2\theta)$ leads immediately to the second, tighter upper bound

$$P(\Sigma_A) \leq \frac{1}{\pi} \int_{\theta=0}^{\pi/2} \left[(\sin^2\theta)(\sin^2\theta + \lambda_{lb} E_c/N_0)^{-y}(\sin^2\theta + \lambda_{ub} E_c/N_0)^{-(1-y)}\right]^d \, \mathrm{d}\theta, \tag{4.8}$$

where $0 \leq y \leq 1$ and satisfies

$$1 = y\lambda_{lb} + (1 - y)\lambda_{ub}.$$

If λ_{lb} and λ_{ub} are chosen such that yd is an integer, partial-fraction expansion of (4.8) results in an alternative expression as the difference of two terms of the form of (3.3). The same approach, followed by application of [18, equation (5.A.3)], results in the difference of two expressions in the form of the Gauss hypergeometric function if yd is not an integer.

CHAPTER 5

BOUNDS ON THE PAIRWISE ERROR-EVENT PROBABILITY FOR THE EXPONENTIALLY CORRELATED CHANNEL

5.1 Minimum-Spacing Error Events

Consider the notional error event of Hamming weight d corresponding to d consecutive code symbols in the code sequence detected by the decoder, which we will refer to as the *minimum-spacing error event* of weight d. (For a particular code and a given value of d, it may be that no such error event is actually possible.) For the ideal periodic-interleaving model and a Rayleigh-fading channel with exponential time correlation, it follows from (2.2) that

$$\mathrm{Cov}(\alpha_i, \alpha_j) = q^{|i-j|}$$

for the minimum-spacing error event .

Let $\Sigma_{ms}(d)$ denote the channel covariance matrix for the minimum-spacing error event of weight d. It is shown in [1] that the eigenvalues of $\Sigma_{ms}(d)$ are bounded by

$$\left(\frac{1-q}{1+q}\right) \leq \lambda_k \leq \left(\frac{1+q}{1-q}\right) \tag{5.1}$$

for all k. (The upper bound also follows from Geršgorin's Theorem.) Moreover, from the implicit solution given in [1] for the eigenvalues of $\Sigma_{ms}(d)$, it follows that the

bounds given by (5.1) are asymptotically tight in d as $d \to \infty$. Thus they are the tightest fixed bounds which are applicable to the minimum-spacing error events for all values of d.

5.2 Other Error Events

Suppose B is the channel covariance matrix for an arbitrary error event of weight d. Let $\hat{B}$ denote the channel covariance matrix for a new notional error event that results from the insertion of an additional zero at some location in the code sequence for the original error event. Therefore, the two matrices can be expressed as

$$B = \begin{pmatrix} B_{11} & B_{12} \\ B_{21} & B_{22} \end{pmatrix} \quad \text{and} \quad \hat{B} = \begin{pmatrix} B_{11} & qB_{12} \\ qB_{21} & B_{22} \end{pmatrix}. \tag{5.2}$$

The eigenvectors of B are denoted $\underline{b}_1, \ldots, \underline{b}_d$ with corresponding eigenvalues $\gamma_1 \leq \ldots \leq \gamma_d$. The eigenvectors of $\hat{B}$ are denoted $\hat{\underline{b}}_1, \ldots, \hat{\underline{b}}_d$ with corresponding eigenvalues $\hat{\gamma}_1 \leq \ldots \leq \hat{\gamma}_d$. Because B and $\hat{B}$ are covariance matrices, both are nonnegative definite.

Lemma 5.1. *All eigenvalues of $\hat{B}$ are within the interval $[\gamma_1, \gamma_d]$.*

Proof: Let

$$f_1(\underline{x}) \triangleq \underline{x}_1^T B_{11} \underline{x}_1 + \underline{x}_2^T B_{22} \underline{x}_2$$

and

$$f_2(\underline{x}) \triangleq \underline{x}_1^T B_{12} \underline{x}_2 + \underline{x}_2^T B_{21} \underline{x}_1,$$

where $\underline{x} = \begin{bmatrix} \underline{x}_1 \\ \\ \underline{x}_2 \end{bmatrix}$, with $\underline{x}_1$ and $\underline{x}_2$ having the appropriate dimensions. Therefore,

$$\underline{x}^T B \underline{x} = f_1(\underline{x}) + f_2(\underline{x}) \text{ and } \underline{x}^T \hat{B} \underline{x} = f_1(\underline{x}) + q f_2(\underline{x}).$$

For any unit-length vector $\underline{x}$, $\hat{\underline{b}}_d^T \hat{B} \hat{\underline{b}}_d \geq \underline{x}^T \hat{B} \underline{x}$. Thus

$$f_1(\hat{\underline{b}}_d) + q f_2(\hat{\underline{b}}_d) = \hat{\underline{b}}_d^T \hat{B} \hat{\underline{b}}_d \geq \tilde{\underline{b}}_d^T \hat{B} \tilde{\underline{b}}_d = f_1(\hat{\underline{b}}_d) - q f_2(\hat{\underline{b}}_d)$$

where

$$\tilde{\underline{b}}_d = \begin{bmatrix} \hat{\underline{b}}_{d,1} \\ \\ -\hat{\underline{b}}_{d,2} \end{bmatrix}.$$

Consequently, $f_2(\hat{\underline{b}}_d) \geq 0$ and

$$\hat{\underline{b}}_d^T B \hat{\underline{b}}_d = f_1(\hat{\underline{b}}_d) + f_2(\hat{\underline{b}}_d) \geq f_1(\hat{\underline{b}}_d) + q f_2(\hat{\underline{b}}_d) = \hat{\underline{b}}_d^T \hat{B} \hat{\underline{b}}_d.$$

Thus,

$$\gamma_d = \underline{b}_d^T B \underline{b}_d \geq \hat{\underline{b}}_d^T B \hat{\underline{b}}_d \geq \hat{\underline{b}}_d^T \hat{B} \hat{\underline{b}}_d = \hat{\gamma}_d.$$

Similarly, $f_2(\hat{\underline{b}}_1) \leq 0$, and consequently, $\gamma_1 \leq \hat{\gamma}_1$. It follows that $\hat{\gamma}_k \in [\hat{\gamma}_1, \hat{\gamma}_d] \subseteq [\gamma_1, \gamma_d]$ for $1 \leq k \leq d$. □

Lemma 5.2. *If the channel is exponentially correlated, the eigenvalues of the channel covariance matrix for each weight-d error event are within the interval* $[\lambda_{ms,1}, \lambda_{ms,d}]$*, where* $\lambda_{ms,1}$ *and* $\lambda_{ms,d}$ *are the minimum and maximum eigenvalues, respectively, of* $\Sigma_{ms}(d)$*.*

Proof: The code sequence of any weight-d error event is obtained from the code sequence of the minimum-spacing error event of weight d by inserting a finite number of zeros into the latter sequence. Through repeated application of Lemma 5.1, it follows that eigenvalues from all weight-d error events fall within the range $[\lambda_{ms,1}, \lambda_{ms,d}]$. □

Lemma 5.3. *If the channel is exponentially correlated, the eigenvalues of the channel covariance matrix for any error event (of any weight) are bounded by (5.1).*

Proof: This follows immediately from Lemma 5.2, because (5.1) applies to $\lambda_{ms,1}$ and $\lambda_{ms,d}$. □

The following two theorems follow directly from Lemma 5.3.

Theorem 5.1. *If the channel is exponentially correlated, the bounds on the pairwise error-event probability in (4.3) and (4.5) hold for all weight-d error events if the eigenvalue bounds in (5.1) are used for* λ_{lb} *and* λ_{ub}*, respectively.*

Theorem 5.2. *If the channel is exponentially correlated, the bounds on the pairwise error-event probability in (4.7) and (4.8) hold for all weight-d error events if the eigenvalue bounds in (5.1) are used for λ_{lb} and λ_{ub}, respectively.*

Stronger results are obtained from further consideration of the relationship between the matrices B and $\hat{B}$. Define the matrix

$$C(u) = (aI + B_{11}) - u^2 B_{12}(aI + B_{22})^c B_{21}$$

as a function of u, where $a \geq 0$ is a constant and $(aI + B_{22})^c$ is the c-inverse of $aI + B_{22}$ defined by

$$(aI + B_{22})(aI + B_{22})^c(aI + B_{22}) = (aI + B_{22}).$$

If $(aI + B_{22})^{-1}$ exists, the matrix $C(u)$ is referred to as the *Schur complement* [14] of $aI + B_{22}$ in the matrix

$$aI + \begin{pmatrix} B_{11} & uB_{12} \\ uB_{21} & B_{22} \end{pmatrix}.$$

Following [19, Theorem 8.2.1],

$$|aI + B| = |aI + B_{22}| \cdot |C(1)| \quad \text{and} \quad |aI + \hat{B}| = |aI + B_{22}| \cdot |C(q)|.$$

Lemma 5.4. $\underline{x}^T C(1)\underline{x} \leq \underline{x}^T C(q)\underline{x}, \quad \forall \underline{x}$

Proof: The matrix B is nonnegative definite because it is a covariance matrix. It follows that $aI + B$ is nonnegative definite; and $C(1)$ is nonnegative definite [19, Theorem 12.2.21]. The matrices $aI+B_{11}$ and $aI+B_{22}$ are nonnegative definite because they are principal submatrices of $aI+B$. Therefore, $(aI+B_{22})^c$ is nonnegative definite and

$$\begin{aligned} \underline{x}^T B_{12}(aI + B_{22})^c B_{21}\underline{x} &= \underline{x}^T B_{21}^T (aI + B_{22})^c B_{21}\underline{x} \\ &= (B_{21}\underline{x})^T (aI + B_{22})^c (B_{21}\underline{x}) \\ &\geq 0, \end{aligned}$$

i.e. $B_{12}(aI + B_{22})^c B_{21}$ is nonnegative definite. But $0 \leq q < 1$; thus,

$$\begin{aligned} \underline{x}^T C(1)\underline{x} &= \underline{x}^T (aI + B_{11})\underline{x} - \underline{x}^T B_{12}(aI + B_{22})^c B_{21}\underline{x} \\ &\leq \underline{x}^T (aI + B_{11})\underline{x} - q^2 \underline{x}^T B_{12}(aI + B_{22})^c B_{21}\underline{x} \\ &= \underline{x}^T C(q)\underline{x}. \end{aligned}$$

□

Lemma 5.5. $|aI + \hat{B}| \geq |aI + B|$ *for any constant* $a \geq 0$.

Proof: Let $\eta_1 \leq \eta_2 \leq \ldots \leq \eta_n$ represent the eigenvalues of $C(1)$, with corresponding eigenvectors $\underline{x}_1, \underline{x}_2, \ldots, \underline{x}_n$, and let $\hat{\eta}_1 \leq \hat{\eta}_2 \leq \ldots, \leq \hat{\eta}_n$ represent the eigenvalues of $C(q)$, with corresponding eigenvectors $\hat{\underline{x}}_1, \hat{\underline{x}}_2, \ldots \hat{\underline{x}}_n$. From Lemma 5.4

and the fact that $\hat{\eta}_n \geq \underline{x}^T C(q)\underline{x}$ for any unit-norm vector $\underline{x}$,

$$\hat{\eta}_n \geq \underline{x}_n^T C(q)\underline{x}_n \geq \underline{x}_n^T C(1)\underline{x}_n = \eta_n.$$

Suppose $1 \leq i \leq n-1$. There is a unit-norm $\underline{x} \in \text{span}\{\underline{x}_n, \underline{x}_{n-1}, \ldots, \underline{x}_{n-i}\}$ such that $\underline{x}$ is orthogonal to $\text{span}\{\hat{\underline{x}}_n, \hat{\underline{x}}_{n-1}, \ldots, \hat{\underline{x}}_{n-i+1}\}$, because

$$\dim\{\underline{x}_n, \underline{x}_{n-1}, \ldots, \underline{x}_{n-i}\} = \dim\{\hat{\underline{x}}_n, \hat{\underline{x}}_{n-1}, \ldots, \hat{\underline{x}}_{n-i+1}\} + 1.$$

It follows that

$$\eta_{n-i} \leq \underline{x}^T C(1)\underline{x} \leq \underline{x}^T C(q)\underline{x} \leq \hat{\eta}_{n-i}.$$

Thus $\hat{\eta}_k \geq \eta_k$, for $1 \leq k \leq n$, and

$$\begin{aligned} |aI + \hat{B}| &= |aI + B_{22}| \cdot |C(q)| \\ &= |aI + B_{22}| \prod_{k=1}^{n} \hat{\eta}_k \\ &\geq |aI + B_{22}| \prod_{k=1}^{n} \eta_k \\ &= |aI + B_{22}| \cdot |C(1)| \\ &= |aI + B|. \end{aligned}$$

□

Theorem 5.3. *If the channel is exponentially correlated and Σ_A is the channel covariance matrix for an error event of weight d, $|aI + \Sigma_A| \geq |aI + \Sigma_{ms}(d)|$.*

Proof: The code sequence of any weight-d error event is obtained from the code

sequence of the minimum-spacing error event of weight d by inserting a finite number of zeros into the latter sequence. The result thus follows from repeated application of Lemma 5.5. □

Theorem 5.4. *If the channel is exponentially correlated and Σ_A is the channel covariance matrix for an error event of weight d, then $|\Sigma_A| \geq |\Sigma_{ms}(d)|$.*

Proof: The result follows immediately from Theorem 5.3 with $a = 0$. □

Note that Theorem 5.4 also follows immediately from [7, equation (11)].

Recall that for the error event with channel covariance matrix Σ, $P(\Sigma)$ denotes its pairwise error-event probability, and $P_C(\Sigma)$ denotes the Chernoff bound on the probability.

Theorem 5.5. *If the channel is exponentially correlated and Σ_A is the channel covariance matrix for an error event of weight d, then $P_C(\Sigma_A) \leq P_C(\Sigma_{ms}(d))$.*

Proof: The result follows immediately from (4.2) and application of Theorem 5.3 with $a = (E_c/N_0)^{-1}$. □

The result of Theorem 5.5 is stated as part of a theorem in [7, Proposition 1] for the more general exponentially correlated Rician-fading channel, but no details of a proof are given therein.

Corollary 5.5.1 follows immediately from Theorem 5.5.

Corollary 5.5.1. *If the channel is exponentially correlated and Σ_A is the channel covariance matrix for an error event of weight d, then $P(\Sigma_A) \leq P_C(\Sigma_{ms}(d))$.*

Note that Theorem 5.1 follows from Corollary 5.5.1 and the results in Chapter 4. The stronger result below also follows from Theorem 5.3.

Theorem 5.6. *If the channel is exponentially correlated and Σ_A is the channel covariance matrix for an error event of weight d, $P(\Sigma_A) \leq P(\Sigma_{ms}(d))$.*

Proof: Application of Theorem 5.3 with $a = \frac{\sin^2\theta}{E_c/N_0}$ yields the inequality

$$\prod_{k=1}^{d}(\sin^2\theta + \lambda_k E_c/N_0) \geq \prod_{k=1}^{d}(\sin^2\theta + \lambda_{ms,k} E_c/N_0)$$

for any θ. It follows that

$$\frac{1}{\pi}\prod_{k=1}^{d}\left[\frac{\sin^2\theta}{\sin^2\theta + \lambda_k E_c/N_0}\right] \leq \frac{1}{\pi}\prod_{k=1}^{d}\left[\frac{\sin^2\theta}{\sin^2\theta + \lambda_{ms,k} E_c/N_0}\right]. \tag{5.3}$$

Integration of each side of (5.3) with respect to θ over the range $[0, \pi/2]$ and comparison of the resulting expressions with (4.6) yields the desired result. □

The result of Theorem 5.6 has been utilized as an (unproven) "folk theorem" in some previous work (such as [20]). Note that Theorem 5.1 and Theorem 5.2 follow from Theorem 5.6 and the results in Chapter 4. Theorem 5.6 applies only to the exponentially correlated channel in general; yet if Σ_1 and Σ_2 are the channel

covariance matrices for two error events in any correlated Rayleigh-fading channel and $|cI + \Sigma_1| \geq |cI + \Sigma_2|$ for all $c \geq 0$, then $P(\Sigma_1) \leq P(\Sigma_2)$.

CHAPTER 6

THE EFFECT OF THE COVARIANCE PARAMETER ON THE PAIRWISE ERROR-EVENT PROBABILITY FOR THE EXPONENTIALLY CORRELATED CHANNEL

Consider an error event with Hamming weight d. Let j_i represent the position of the ith "one" in the code sequence of the error event. The spacing between consecutive "ones" is represented by the vector $\underline{\Delta} = (\Delta_1, \Delta_2, \ldots, \Delta_{d-1})$, where $\Delta_i = j_{i+1} - j_i$. Let $\Sigma_{\underline{\Delta}}(q)$ represent the covariance matrix corresponding to this error event if the covariance parameter is q, $0 \leq q \leq 1$.

Theorem 6.1. *If the channel is exponentially correlated and $\underline{\Delta}$ is the spacing vector for an error event of Hamming weight d, then $P_C(\Sigma_{\underline{\Delta}}(q_1)) \leq P_C(\Sigma_{\underline{\Delta}}(q_2))$ for $q_1 \leq q_2$.*

Proof: Let $B(1) = \Sigma_{\underline{\Delta}}(q_2)$. For $1 \leq i \leq d-1$, let $B_{11}(i)$ denote the upper left i-by-i submatrix of $B(i)$, and define $\hat{B}(i)$ based on $B(i)$ according to (5.2) with $q = (q_1/q_2)^{\Delta_1}$. From Lemma 5.5 with $a = (E_c/N_0)^{-1}$, $P_C(B(i)) \geq P_C(\hat{B}(i))$. But $\hat{B}(d-1) = \Sigma_{\underline{\Delta}}(q_1)$; thus $P_C(\Sigma_{\underline{\Delta}}(q_1)) \leq P_C(\Sigma_{\underline{\Delta}}(q_2))$. □

The result of Theorem 6.1 is stated as the second part of a theorem in [7, Proposition 1] for the more general exponentially correlated Rician-fading channel; yet a new, stronger result also follows from Theorem 6.1.

Theorem 6.2. *If the channel is exponentially correlated and* $\underline{\Delta}$ *is the spacing vector for an error event of Hamming weight* d*, then* $P(\Sigma_{\underline{\Delta}}(q_1)) \leq P(\Sigma_{\underline{\Delta}}(q_2))$ *for* $q_1 \leq q_2$*.*

Proof: The same iterative argument is followed as in the proof of Theorem 6.1, except that Lemma 5.5 is applied with $a = \frac{\sin^2\theta}{E_c/N_0}$ at each step. Integration of each side of the resulting inequality with respect to θ over the range $[0, \pi/2]$, as in the proof of Theorem 5.6, yields the desired result. □

Recall that the covariance parameter is $q = \exp(-2\pi m D_T)$. For a given error event and a fixed interleaving depth, increasing the normalized Doppler spread will thus decrease both the pairwise error-event probability and its Chernoff bound. Similarly, increasing the interleaving depth will decrease both the pairwise error-event probability and its Chernoff bound.

CHAPTER 7

BOUNDS ON THE PROBABILITY OF BIT ERROR FOR THE EXPONENTIALLY CORRELATED CHANNEL

The standard union bound on the probability of bit error is given by

$$P_b \leq \sum_{\underline{c} \in \mathcal{C}} i(\underline{c}) P(\underline{c}) \tag{7.1}$$

where $\mathcal{C}$ is the infinite set of code sequences of the code and $i(\underline{c})$ is the weight of the information sequence that maps to $\underline{c}$ (i.e., the code sequence's *information weight*). The infinite series can not be expressed in a closed form, but a closed-form upper bound on it can be obtained using the code's transfer function.

The transfer function of the convolutional code, denoted $T(D, I)$, is a power series in the indeterminate variables D and I in which the summand $a_{j,k} D^j I^k$ indicates that the code has $a_{j,k}$ distinct error events of Hamming weight j and information weight k [21]. Any bound on the pairwise error-event probability that is a linear combination of geometric functions of the Hamming weight of the error event can be used in conjunction with the transfer function to obtain a closed-form upper bound on the union bound on the probability of bit error (which is thus an upper bound on the actual probability of bit error).

7.1 Rational-Polynomial Bounds

If the bound $g(E_c/N_0)$ on the pairwise error-event probability is a geometric function of the Hamming weight, the resulting transfer-function bound for a code of rate b/n is given by

$$P_b \leq \frac{1}{2b} \left. \frac{\mathrm{d}T(D,I)}{\mathrm{d}I} \right|_{D=g(E_c/N_0),I=1} . \tag{7.2}$$

The bound in (4.3) and the result of Theorem 5.1 together yield the transfer-function bound of (7.2) with

$$g(E_c/N_0) = \left[1 + \left(\frac{1-q}{1+q}\right) \frac{E_c}{N_0}\right]^{-1} \tag{7.3}$$

for the exponentially correlated Rayleigh-fading channel. A tighter transfer-function bound for the same channel is obtained by using (4.5) instead of (4.3). From (5.1) it follows that (4.5) is true for $y = (1+q)/2$. This results in the transfer-function bound of (7.2) with

$$g(E_c/N_0) = \left\{ \left[1 + \left(\frac{1-q}{1+q}\right) \frac{E_c}{N_0}\right]^{(1+q)/2} \left[1 + \left(\frac{1+q}{1-q}\right) \frac{E_c}{N_0}\right]^{(1-q)/2} \right\}^{-1} . \tag{7.4}$$

7.2 Integral Bounds

The approach in the previous section can also be applied to the integrand in the integral-form bounds derived in Chapter 4 for the pairwise error-event probability. In each instance, the resulting bound on the probability of bit error has the form of a single-dimensional proper integral with a rational-polynomial integrand. Specifically,

for a code of rate b/n it is given by

$$P_b \leq \frac{1}{b\pi} \int_{\theta=0}^{\pi/2} \left. \frac{\mathrm{d}T(D,I)}{\mathrm{d}I} \right|_{D=g(E_c/N_0,\theta),I=1} \mathrm{d}\theta, \tag{7.5}$$

where $g(E_c/N_0, \theta)$ is determined by the particular geometric-form bound used for the pairwise error-event probability. The use of (4.7) results in the transfer-function bound (7.5) with

$$g(E_c/N_0, \theta) = [\sin^2 \theta] \Big/ \left[\sin^2 \theta + \left(\frac{1-q}{1+q} \right) \frac{E_c}{N_0} \right] \tag{7.6}$$

for the exponentially correlated Rayleigh-fading channel. A tighter bound on the probability of bit error for the same channel is obtained by using (4.8). This results in the transfer-function bound of (7.5) with

$$\begin{aligned} g(E_c/N_0) &= [\sin^2 \theta] \\ &\quad \times \left\{ \left[\sin^2 \theta + \left(\frac{1-q}{1+q} \right) \frac{E_c}{N_0} \right]^{(1+q)/2} \left[\sin^2 \theta + \left(\frac{1+q}{1-q} \right) \frac{E_c}{N_0} \right]^{(1-q)/2} \right\}^{-1}. \end{aligned} \tag{7.7}$$

7.3 Term-by-Term Corrections

The transfer-function bounds in (7.2) and (7.5) are looser than the union bound (7.1), but the former are amenable to exact evaluation whereas the latter is not. A closed-form expression with accuracy closer to that of the union bound can be obtained by replacing the summands in (7.2) or (7.5) for a finite subset of the error

events with the exact closed-form expressions for those error events. This "term-by-term correction" [22] of the transfer-function bound has been applied previously to transfer-function bounds using standard Chernoff bounds on the pairwise error-event probability for exponentially correlated Rician fading and non-coherent communications [23]. The approach focuses on error events of the lowest Hamming weights, since they dominate the performance at a large signal-to-noise ratio and are the easiest to catalog exhaustively. Term-by-term correction for the set of error events of a given Hamming weight requires knowledge of the details of the code sequence associated with each error event (in order to determine the eigenvalues of the corresponding channel covariance matrix) in addition to its information weight.

A term-by-term correction of the rational-polynomial bound in (7.2) for the code sequences in the set S is given by

$$P_b \leq \frac{1}{2b} \left. \frac{\mathrm{d}T(D,I)}{\mathrm{d}I} \right|_{D=g(E_c/N_0),I=1} + \frac{1}{b} \sum_{\underline{c} \in S} i(\underline{c}) \left(P(\underline{c}) - \frac{1}{2}[g(E_c/N_0)]^{w(\underline{c})} \right) \tag{7.8}$$

where $w(\underline{c})$ denotes the Hamming weight of $\underline{c}$. As in Section 7.1, either (7.3) or (7.4) can be used for $g(E_c/N_0)$, with the latter of the two yielding the tighter upper bound. Similarly, a term-by-term correction of the integral bound in (7.5) for codewords of

the set S is given by

$$P_b \leq \frac{1}{b\pi} \int_{\theta=0}^{\pi/2} \left(\left. \frac{\mathrm{d}T(D,I)}{\mathrm{d}I} \right|_{D=g(E_c/N_0,\theta),I=1} - \sum_{\underline{c} \in S} i(\underline{c}) [g(E_c/N_0)]^{w(\underline{c})} \right) \mathrm{d}\theta + \frac{1}{b} \sum_{\underline{c} \in S} i(\underline{c}) P(\underline{c}). \quad (7.9)$$

Either (7.6) or (7.7) can be used for $g(E_c/N_0)$, with the latter of the two yielding the tighter upper bound.

Term-by-term corrections can be computationally intensive, especially for a code with a large constraint length. Correction for error events of the several lowest Hamming weights can require consideration of a large number of error events. The exact structure of each corresponding code sequence (in particular, the placement of non-zero bits within the code sequence) cannot be obtained analytically even from the three-variable complete path-weight enumerator [21] of the code. Instead a search of the code trellis is required. Moreover, separate calculations are required to determine the eigenvalues for the channel covariance matrix and the resulting pairwise error-event probability for each low-weight error event.

This computational burden can be largely eliminated for exponentially correlated Rayleigh fading by using a somewhat weaker correction to the transfer-function bound. By Theorem 5.6, the bounds in (7.8) and (7.9) can be weakened if $P(\underline{c})$ for each $\underline{c} \in S$ is replaced with the pairwise error-event probability for the minimum-spacing error event of the same Hamming weight as $\underline{c}$. Applying this approach to (7.8)

for term-by-term correction for the error events of weights d_{free} through N results in

$$P_b \leq \frac{1}{2b} \left. \frac{\mathrm{d}T(D,I)}{\mathrm{d}I} \right|_{D=g(E_c/N_0),I=1} + \frac{1}{b} \sum_{k=d_{free}}^{N} B_k \left(P(\underline{c}_{ms}(k)) - \frac{1}{2}[g(E_c/N_0)]^k \right), \quad (7.10)$$

where $\underline{c}_{ms}(k)$ is a sequence of k ones and B_k is the sum of the information weights of all Hamming-weight-k error events. The term B_k is often tabulated for good codes for low-weight error events; alternatively, it can be obtained from polynomial long division of $\left. \frac{\mathrm{d}T(D,I)}{\mathrm{d}I} \right|_{I=1}$. Thus, a computer search to determine the details of each error event in the set S is not required. Furthermore, the pairwise error-event probability need be calculated only once for each Hamming weight for which the correction is applied. Applying the same approach to (7.9) for term-by-term correction for the error events of weights d_{free} through N results in

$$P_b \leq \frac{1}{b\pi} \int_{\theta=0}^{\pi/2} \left(\left. \frac{\mathrm{d}T(D,I)}{\mathrm{d}I} \right|_{D=g(E_c/N_0,\theta),I=1} - \sum_{k=d_{free}}^{N} B_k [g(E_c/N_0)]^k \right) \mathrm{d}\theta + \frac{1}{b} \sum_{k=d_{free}}^{N} B_k P(\underline{c}). \quad (7.11)$$

CHAPTER 8

NUMERICAL RESULTS FOR THE EXPONENTIALLY CORRELATED CHANNEL

In this chapter, simulation results and bounds are compared by considering the performance of a system using the "NASA standard" constraint-length-seven, rate-1/2 convolutional code [24] over the exponentially correlated Rayleigh-fading channel.

8.1 Comparison of Block Interleaving with the Ideal Periodic-Interleaving Model

The ideal periodic interleaver represents an idealization of interleaving in a real communication system in that the relationship given in (2.2) cannot be realized for all j and k for any interleaver design. The ideal periodic-interleaving model often results in performance analysis that is more tractable than if a block interleaver is considered, however. Consideration of ideal periodic interleaving is also sufficient for obtaining many useful insights into the design and performance of communication systems.

Consider a p-by-m rectangular block interleaver into which code symbols are written by rows and out of which they are read by columns. The column dimension m thus corresponds to the designed interleaving depth. The row dimension p determines the maximum span of consecutive code symbols into the interleaver over which the ideal periodic-interleaving model correctly represents the fading to which the code symbols are subjected. Any span of more than p consecutive code symbols results

in some pairs of symbols that are subjected to more highly correlated fading than is predicted by the ideal periodic-interleaving model. Thus for a given block size $p \cdot m$, the choice of the dimensions represents a tradeoff between the designed interleaving depth and the length of code-symbol sequences over which the designed interleaving depth is achieved. It also affects the accuracy of the ideal periodic-interleaving model.

Both of these phenomena are illustrated in Figure 8.1, which compares simulation results for a block size of 1200 binary code symbols and a normalized Doppler spread of $D_T = 10^{-3}$. Results are shown for systems with both ideal periodic interleaving and block interleaving. Block interleavers with dimensions of 120-by-10, 30-by-40, and 10-by-120 are considered, along with the corresponding ideal periodic-interleaving models with interleaving depths of 10, 40, and 120 bits, respectively.

The 120-by-10 block interleaver has a designed interleaving depth ($m = 10$) that is small; thus it provides only limited time diversity as protection against error events of any span. The 10-by-120 block interleaver has a large designed interleaving depth ($m = 120$). The designed depth is not achieved for even the shortest-span error events with this interleaver, however, due to the small row dimension ($p = 10$). The 30-by-40 block interleaver achieves a better balance between these two objectives than either of the other two block interleavers, and it results in better performance than either of them.

The ideal periodic-interleaving model does not account for the effect of the finite row dimension, however, and thus the performance for that model improves monotonically as the interleaving depth is increased. The performance with the block

interleaver and the performance with the ideal periodic-interleaving model are thus in closest agreement when the row dimension of the block interleaver is much larger than the minimum error-event span of the code. As the row dimension is decreased (and the designed interleaving depth is increased) for a fixed block size, the difference in performance for the two interleaver models increases. In each instance, better performance is predicted with the ideal periodic-interleaving model than is achieved with the block interleaver.

The difference between performance using a block interleaver and the performance obtained with the ideal periodic-interleaving model is also affected by the Doppler spread, as illustrated in Figure 8.2. The block interleaver has dimensions 24-by-24, and the ideal periodic interleaver has an interleaving depth of $m = 24$. The performance is shown for independent Rayleigh fading and for correlated Rayleigh fading with five different values of the Doppler spread: $D_T = 10^{-3}$, $D_T = 10^{-5}$, $D_T = 10^{-7}$, $D_T = 10^{-9}$, and $D_T = 0$ (i.e., *flat fading*). The performance with block interleaving and the performance with ideal periodic interleaving are in agreement for either extreme of the Doppler spread (independent fading or flat fading); in fact, the interleaving technique (or the absence of interleaving) is irrelevant to the system's performance in either of the two instances. The performance differs using the two interleavers for any intermediate value of Doppler spread, however, and in each instance the performance with block interleaving is poorer than is predicted by the ideal periodic-interleaving model. The difference is small for very small or moderate-to-large Doppler spreads and is greatest for moderately small values of the Doppler

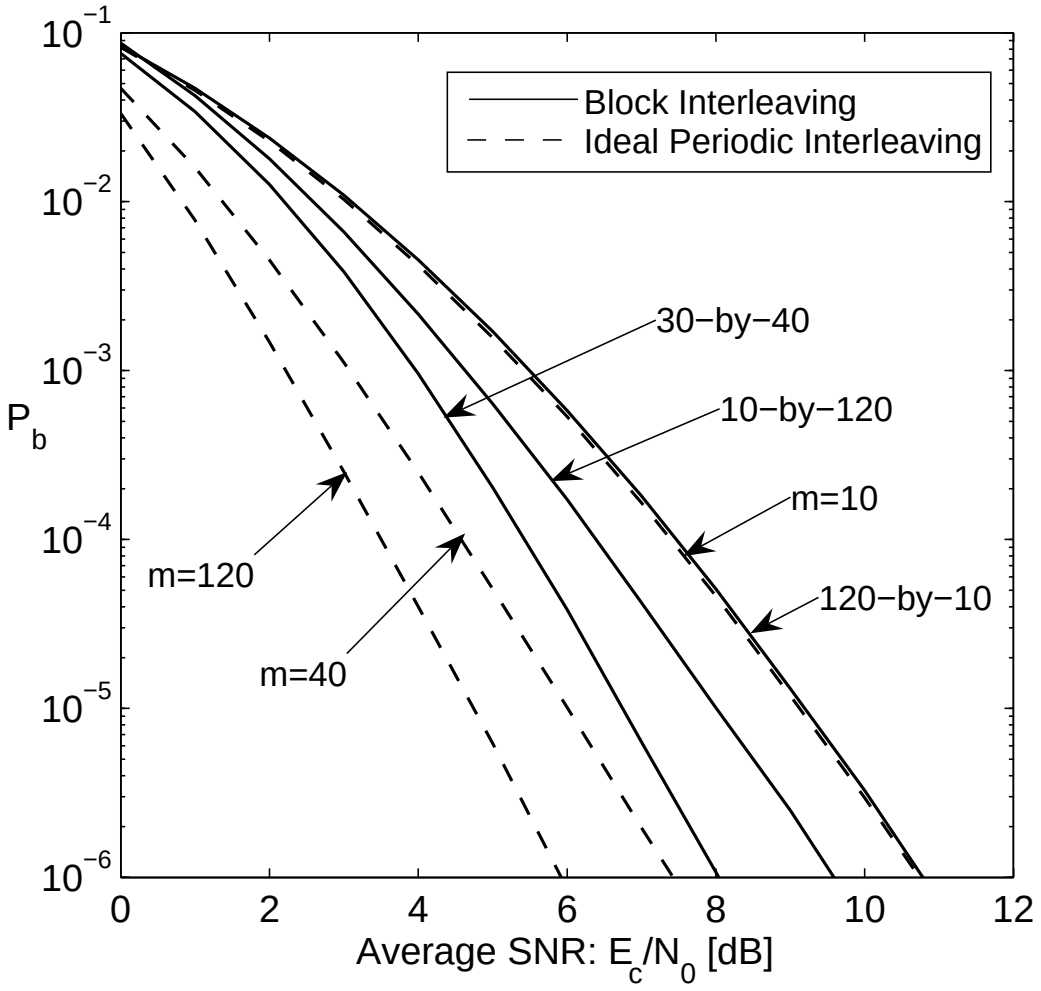

Figure 8.1: Simulations with ideal periodic and block interleaving for the NASA standard, $K = 7$, rate-1/2 convolutional code for $D_T = 10^{-3}$ and a block size of 1200 (code) bits.

spread.

8.2 Accuracy of the Bounds for the Ideal Periodic-Interleaving Model

The accuracy of the three (new) closed-form bounds developed in this thesis is compared with the accuracy of the closed-form bound of (7.2) and (7.3) (i.e., using the result from [7]). The latter bound is referred to as the *rational-polynomial bound*. The new bound using (7.2) and (7.4) is referred to as the *tighter rational-polynomial bound*, the new bound using (7.5) and (7.6) is referred to as the *integral bound*, and the new bound using (7.5) and (7.7) is referred to as the *tighter integral bound*. Results are shown in Figures 8.3-8.5 for a system using an ideal periodic interleaver with a depth of 24 bits. Each figure contains results for a different fading rate.

Figure 8.3 shows the bounds and simulation results for the probability of bit error as a function of E_c/N_0 for a channel with a normalized Doppler spread of $D_T = 10^{-1}$. For this fading rate, the rational-polynomial bound from (7.3) and the integral bound from (7.6) are nearly indistinguishable from their tighter counterparts from (7.4) and (7.7), respectively. The integral bounds are much tighter than the rational-polynomial bounds, however. The two integral bounds differ by 0.1 dB from the actual performance if the probability of bit error is 10^{-4}, for example, whereas the two rational-polynomial bounds differ from the actual performance by 0.9 dB.

Figure 8.4 shows analogous results for a more slowly time-varying fading channel for which $D_T = 10^{-2}$. Greater differences between the bounds occur for this channel than for the channel with the larger Doppler spread. If the probability of bit error is

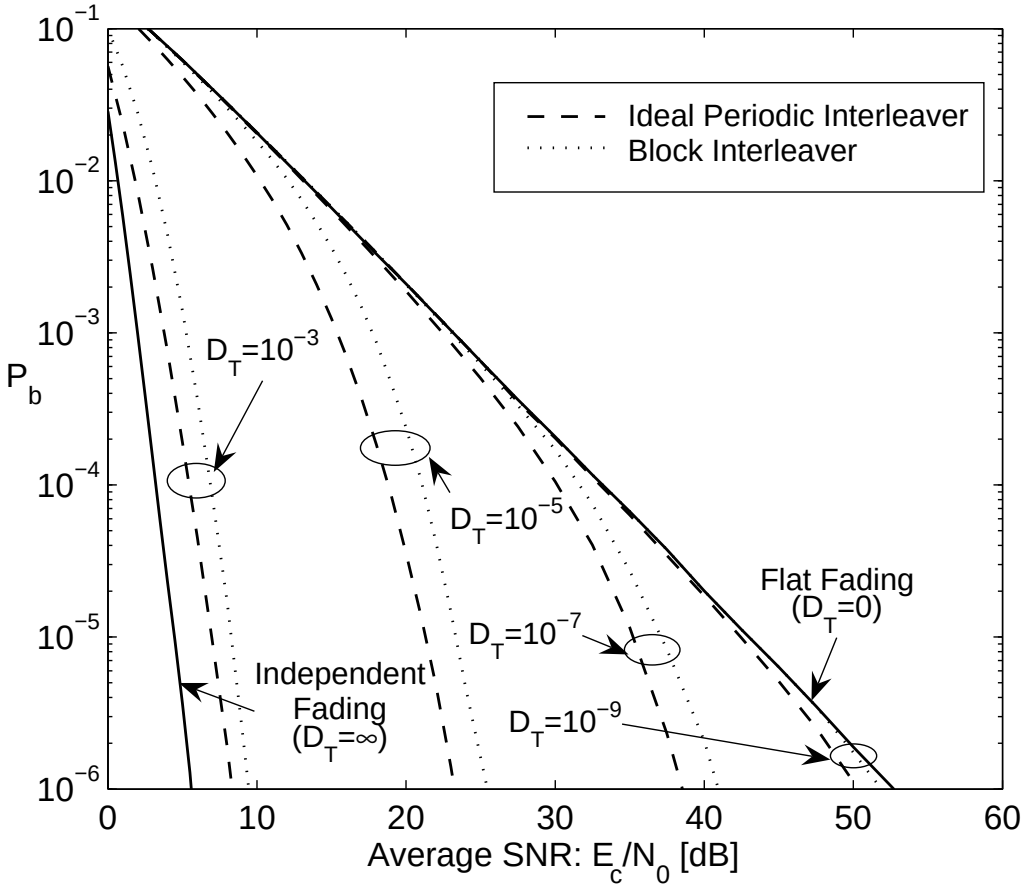

Figure 8.2: Simulations with ideal periodic and block interleaving for the NASA standard, $K = 7$, rate-1/2 convolutional code for various normalized Doppler spreads and an interleaving depth of 24 bits.

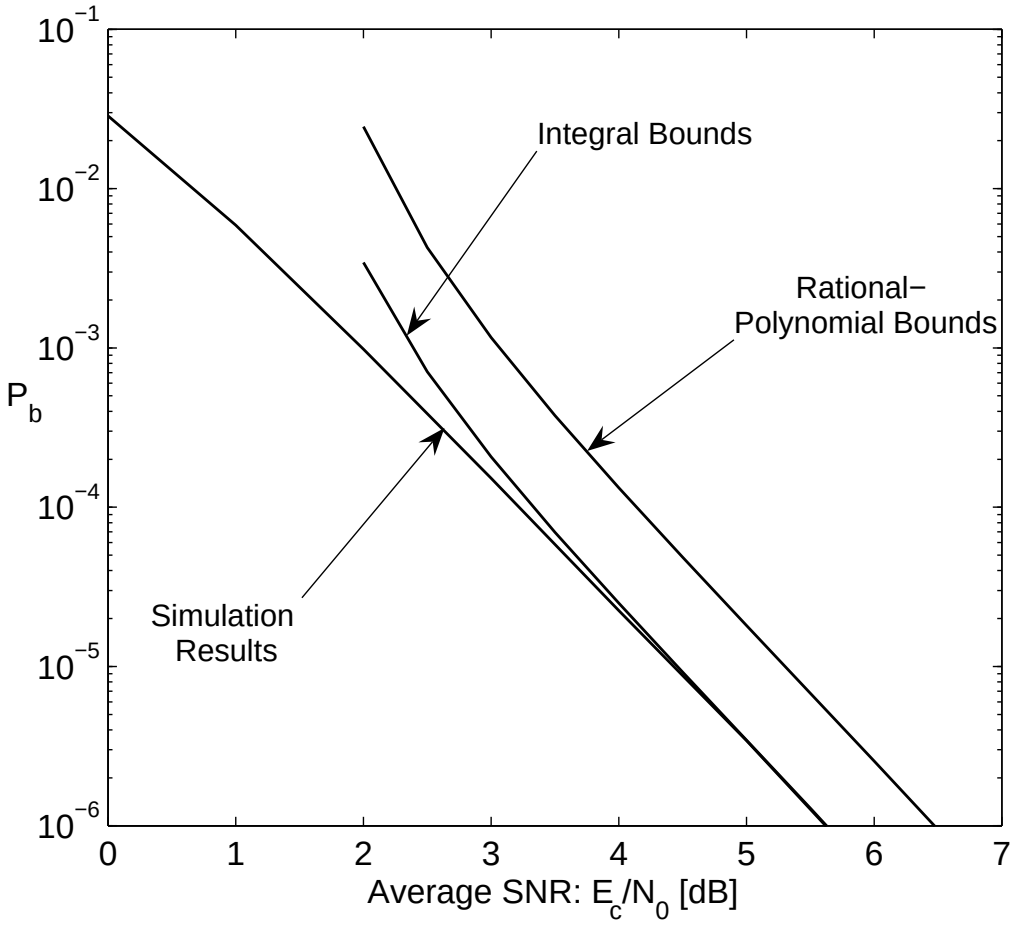

Figure 8.3: Bounds and simulation results for the NASA standard, $K = 7$, rate-1/2 convolutional code for $D_T = 10^{-1}$ and an interleaving depth of 24 bits.

10^{-4}, the rational-polynomial bound from (7.3) differs from the actual performance by 2.8 dB, while the tighter rational-polynomial bound from (7.4) is within 1.2 dB of the actual performance. For the same probability of bit error, the integral bound from (7.6) and tighter integral bound from (7.7) differ from the actual performance by 2.0 dB and 0.4 dB, respectively.

Figure 8.5 shows results for the smaller normalized Doppler spread of $D_T = 10^{-3}$. It can be seen that the bounds are much less accurate in this case than for the two higher Doppler spreads considered in Figures 8.3 and 8.4. For a probability of bit error of 10^{-4}, the rational-polynomial bound from (7.3) differs from the actual performance by 9.9 dB if $D_T = 10^{-3}$, whereas the tighter rational-polynomial bound from (7.4) is within 7.8 dB of the actual performance. For the same probability of bit error, the integral bound from (7.6) and tighter integral bound from (7.7) differ from the actual performance by 9.1 dB and 6.9 dB, respectively.

As described in Section 7.3, the accuracy of the bounds can be improved using term-by-term corrections. Figure 8.6 illustrates the value of the corrections for the system with an interleaving depth of 24 bits over the channel with a normalized Doppler spread $D_T = 10^{-3}$ (the same parameters used for Figure 8.5). Term-by-term corrections to the integral bound and tighter integral bound for all error events with Hamming weights 10, 12, and 14 (the lowest three weights for this code) are included based on (7.9), along with their "uncorrected" counterparts. If the probability of bit error is 10^{-4}, an improvement of 0.4 dB is achieved by applying the term-by-term corrections to the integral bound. For the same probability of bit error, there is

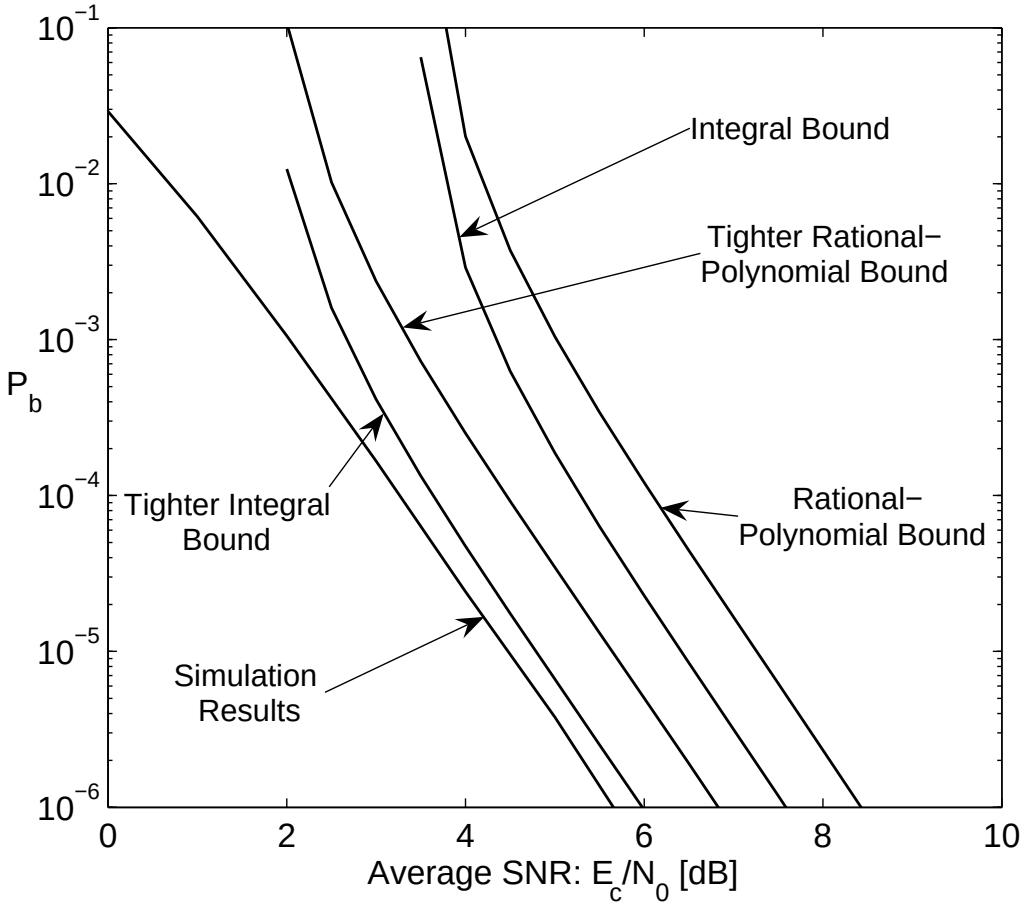

Figure 8.4: Bounds and simulation results for the NASA standard, $K = 7$, rate-1/2 convolutional code for $D_T = 10^{-2}$ and an interleaving depth of 24 bits.

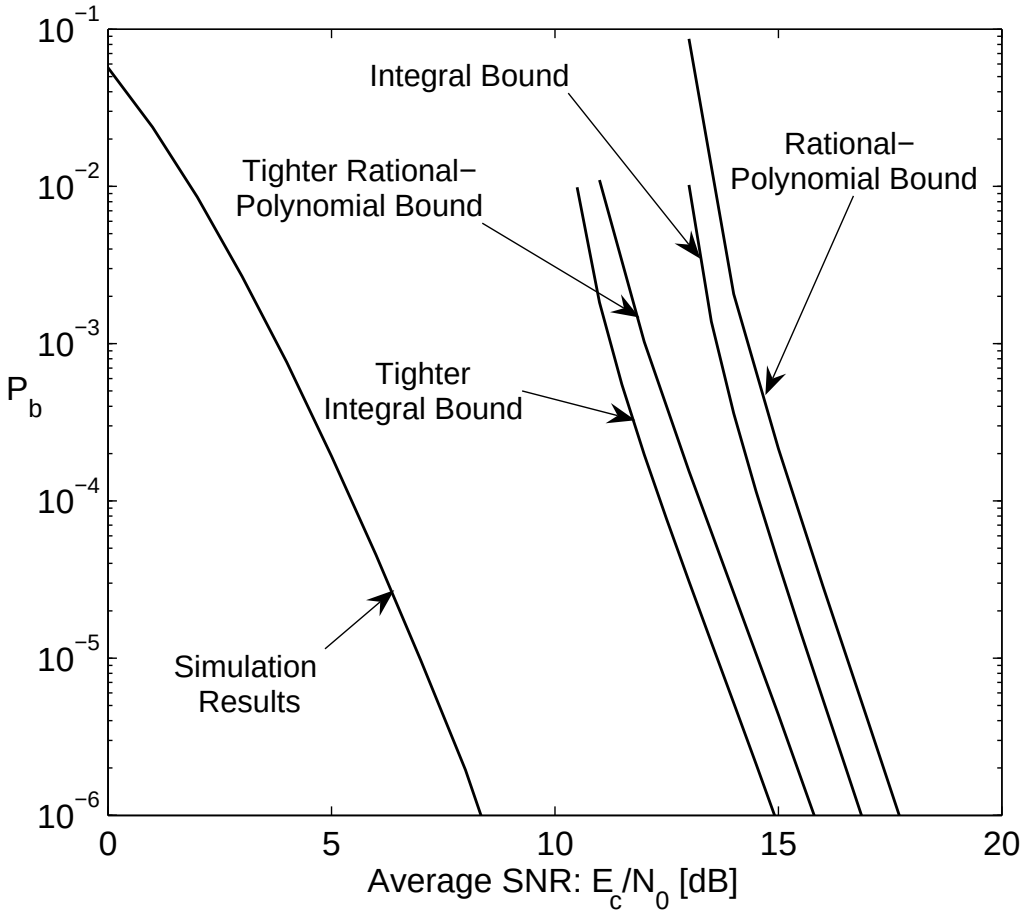

Figure 8.5: Bounds and simulation results for the NASA standard, $K = 7$, rate-1/2 convolutional code for $D_T = 10^{-3}$ and an interleaving depth of 24 bits.

an improvement of 0.5 dB if the term-by-term corrections are applied to the tighter integral bound. For this interleaving depth and Doppler spread, moreover, the looser term-by-term corrections in (7.11) yield results so close to those in (7.9) that the two are nearly indistinguishable when plotted using the scale of Figure 8.6.

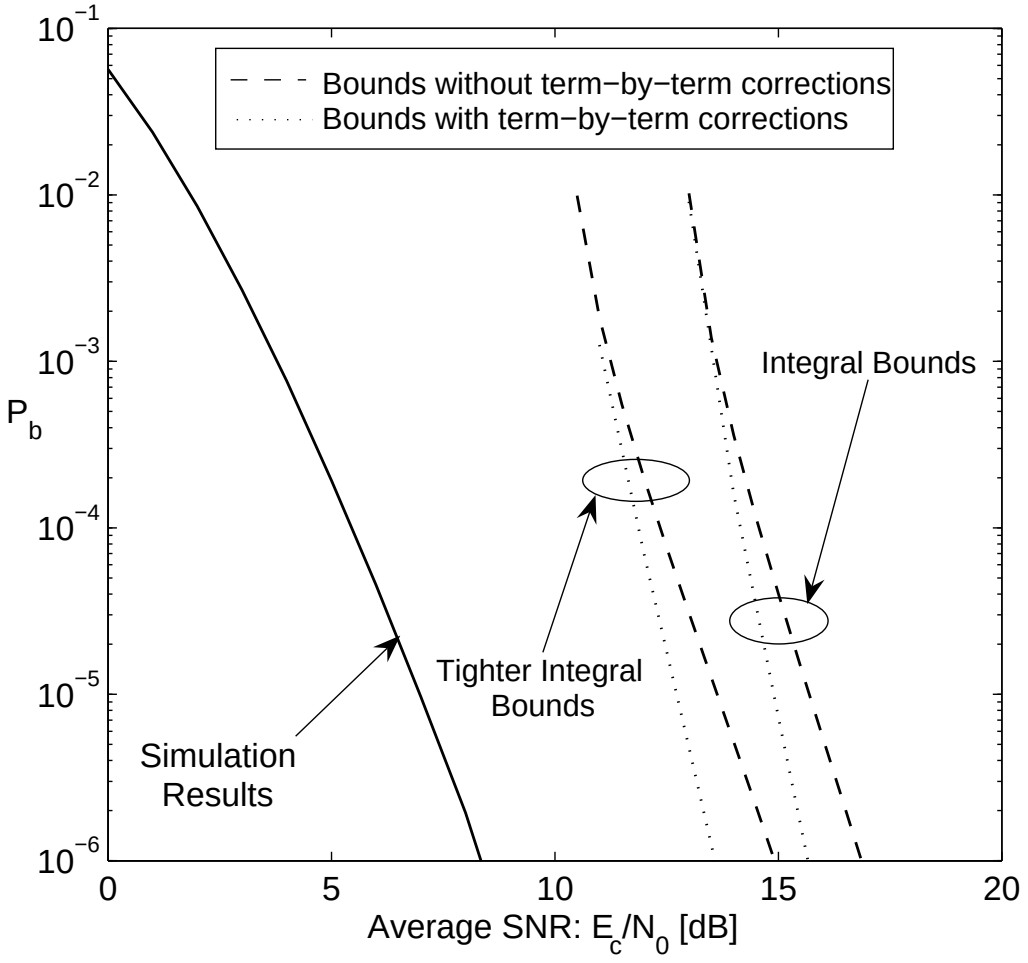

Figure 8.6: Term-by-term corrections of integral bounds for the NASA standard, $K = 7$, rate-1/2 convolutional code, $D_T = 10^{-3}$, and an interleaving depth of 24 bits

CHAPTER 9

CONCLUSION

Convolutional coding and maximum-likelihood decoding are considered for communications over a correlated Rayleigh-fading channel. New bounds on the pairwise error-event probability are developed for a general correlated channel with ideal periodic interleaving in terms of upper and lower bounds on the eigenvalues of the channel covariance matrix. These results are applied to the exponentially correlated channel, and the relationship between the spacing of the erroneous code symbols in an error event and its pairwise error-event probability is explored. Most notably, it is shown that the minimum-spacing error event of a given Hamming weight results in the largest pairwise error-event probability among all error events of that weight.

The bounds on the pairwise error-event probability for the exponentially correlated channel are then used to develop three new closed-form bounds on the probability of bit error. It is shown that the new bounds can be as much as several decibels tighter than previously developed bounds. Term-by-term corrections are shown to improve the accuracy of the bounds, but their evaluation can be quite computationally intensive. A weaker correction is also considered, which eliminates much of the computational burden and yields an improvement in the accuracy of the bounds very close to that of the more traditional term-by-term corrections.

REFERENCES

[1] J. Pierce and S. Stein, "Multiple diversity with nonindependent fading," *Proc. IRE*, vol. 48, pp. 89–104, Jan 1960.

[2] J. Jootar, J. Zeidler, and J. Proakis, "Performance of convolutional codes with finite-depth interleaving and noisy channel estimates," *IEEE Trans. Commun.*, vol. 54, pp. 1775–1786, Oct 2006.

[3] A. Viterbi and J. Omura, *Principles of Digital Communication and Coding*. McGraw-Hill, 1979.

[4] J. Modestino and S. Mui, "Convolutional code performance in the Rician fading channel," *IEEE Trans. Commun.*, vol. 24, pp. 592–606, June 1976.

[5] R. Cideciyan and E. Eleftheriou, "New bounds on convolutional code performance over fading channels." Trondheim, Norway: Intl. Symp. on Inform. Theory, June 1994, p. 270.

[6] F. Gagnon and D. Haccoun, "Bounds on the error performance of coding for nonindependent Rician-fading channels," *IEEE Trans. Commun.*, vol. 40, pp. 351–360, Feb 1992.

[7] G. Kaplan and S. Shamai, "Achievable performance over the correlated Rician channel," *IEEE Trans. Commun.*, vol. 42, pp. 2967–2978, Nov 1994.

[8] C. Tellambura, "Evaluation of the exact union bound for trellis-coded modulations over fading channels," *IEEE Trans. Commun.*, vol. 44, pp. 1693–1699, Dec 1996.

[9] M. Simon and D. Divsalar, "Some new twists to problems involving the Gaussian probability integral," *IEEE Trans. Commun.*, vol. 46, pp. 200–210, Feb 1998.

[10] P. A. Bello and B. D. Nelin, "The influence of fading spectrum on the binary error probabilities of incoherent and differentially coherent matched-filter receivers," *IRE Trans. Commun. Syst.*, vol. CS-10, no. 2, pp. 160–168, June 1962.

[11] R. Garello, G. Montorsi, S. Benedettom, and G. Cancellieri, "Interleaver properties and their applications to the trellis complexity analysis of turbo codes," *IEEE Trans. Commun.*, vol. 49, pp. 793–806, May 2001.

[12] G. Forney, Jr., "Burst-correcting codes for the classic bursty channel," *IEEE Trans. Commun. Technol.*, vol. COM-19, pp. 772–781, Oct 1973.

[13] G. L. Turin, "On optimal diversity reception II," *IRE Trans. Commun. Syst.*, vol. CS-10, no. 1, pp. 22–31, March 1962.

[14] P. Lancaster and M. Tismenetsky, *The Theory of Matrices*, 2nd ed. Academic Press, 1985.

[15] T. M. Cover and J. A. Thomas, *Elements of Information Theory*, 2nd ed. John Wiley & Sons, 2006.

[16] V. Veeravalli, "On performance analysis for signaling on correlated fading channels," *IEEE Trans. Commun.*, vol. 49, pp. 1879–1883, Nov 2001.

[17] A. Chindapol and J. Ritcey, "Performance analysis of coded modulation with generalized selection combining in Rayleigh fading," *IEEE Trans. Commun.*, vol. 51, pp. 1348– 1357, Aug 2003.

[18] M. K. Simon and M.-S. Alouini, *Digital Communication over Fading Channels*, 2nd ed. Wiley-IEEE Press, 2004.

[19] F. A. Graybill, *Matrices with Applications in Statistics*, 2nd ed. Wadsworth International, 1983.

[20] C. Tellambura and V. Bhargava, "Error performance of MPSK trellis-coded modulation over nonindependent Rician fading channels," *IEEE Trans. Veh. Technol.*, vol. 47, pp. 152–162, Feb 1998.

[21] A. J. Viterbi, "Convolutional codes and their performance in communication systems," *IEEE Trans. Commun.*, vol. COM-19, no.5, pp. 751–772, Oct 1971.

[22] W. E. Stark, "Coding for frequency-hopped spread-spectrum communication with partial-band interference, part II: Coded performance," *IEEE Trans. Commun.*, vol. 33, pp. 1045–1057, Oct 1985.

[23] D. Noneaker and C. Frank, "The effect of finite interleaving depth on the performance of convolutional codes in Rician-fading channels." Trondheim, Norway: Intl. Symp. on Inform. Theory, June 1994, p. 29.

[24] Consultative Committee for Space Data Systems, "Recommendation for space data systems standard, telemetry channel coding," *Blue Book*, vol. CCSDS 101.0-B-2, issue 2, Jan. 1987.